

Supporting Information

Ascorbic acid functionalized CdS-ZnO core-shell nanorods with hydrogen spillover for greatly enhanced photocatalytic H₂ evolution and outstanding photostability

Guotai Sun^{a,b,1}, Bing Xiao^{a,1}, Hong Zheng^a, Jian-Wen Shi^{a,*}, Siman Mao^a, Chi He^c, Zhihui Li^a,
Yonghong Cheng^a

¹ The authors contribute equally to this work

^a*Center of Nanomaterials for Renewable Energy, State Key Laboratory of Electrical Insulation and Power Equipment, School of Electrical Engineering, Xi'an Jiaotong University, Xi'an 710049, China.*

^b*Center for Nano Energy Materials, State Key Laboratory of Solidification Processing, School of Materials Science and Engineering, Northwestern Polytechnical University, Xi'an 710072, China.*

^c*State Key Laboratory of Multiphase Flow in Power Engineering, School of Energy and Power Engineering, Xi'an Jiaotong University, Xi'an 710049, China.*

Corresponding author:

Jian-Wen Shi, E-mail: jianwen.shi@mail.xjtu.edu.cn

1. Materials

Sodium sulfite (Na_2SO_3), sodium sulfate (Na_2SO_4), sodium hydroxide (NaOH) and thiourea ($\text{CH}_4\text{N}_2\text{S}$) were obtained from Sinopharm Chemical Reagent Co., Ltd. Cadmium chloride ($\text{CdCl}_2 \cdot 2.5\text{H}_2\text{O}$) was obtained from Tianjin Kermel Chemical Reagent Co., Ltd. Sodium sulfide ($\text{Na}_2\text{S} \cdot 9\text{H}_2\text{O}$) was received from Tianjin Tianli Chemical Reagent Co., Ltd. Zinc chloride (ZnCl_2) was ordered from Tianjin Shengao Chemical Reagent Co., Ltd. Ascorbic acid (AA) was ordered from Guangdong Guanghua sci-tech Co., Ltd. Ammonia solution ($\text{NH}_3 \cdot \text{H}_2\text{O}$) was purchased from Shanghai Aladdin Bio-Chem Technology Co., Ltd. All the reagents were analytically pure and used directly without further purification. Distilled water with a resistivity of $18.2 \text{ M}\Omega \cdot \text{cm}$ was used throughout the experiments.

2. The measurement and calculation of apparent quantum efficiency

The apparent quantum efficiency (AQE) of the CSZ_{0.5} sample was measured under the same photocatalytic reaction condition (20 mg of catalysts in 50 mL of aqueous solution of 0.35 M Na₂S and 0.25 M Na₂SO₃) using 300 W Xenon lamp assembled with different band-pass filters of wavelengths. The AQE was calculated by the equation as follows:

$$\begin{aligned}AQE &= \frac{\text{number of reacted electrons}}{\text{number of incident photons}} \times 100 \% \\ &= \frac{\text{number of evolved } H_2 \text{ molecules} \times 2}{\text{number of incident photons}} \times 100 \% \\ &= \frac{n_{H_2} \times N_A \times 2}{E\lambda/hc} \times 100 \%\end{aligned}$$

For instance, the above equation can be utilized to make the following calculation for the AQE at 365 nm wavelength with the requisite experimental data, including the power density of Xenon lamp at 365 nm (1.834 mW/cm²), the effective area under irradiation light (28.26 cm²) and the amount of generated hydrogen in 2 h (196.10 μmol).

$$\begin{aligned}AQE &= \frac{196.10 \times 10^{-6} \times 6.02 \times 10^{23} \times 2}{1.834 \times 10^{-3} \times 28.26 \times 3600 \times 2 \times 365 \times 10^{-9} / (6.626 \times 10^{-34} \times 3 \times 10^8)} \times 100 \% \\ &= 34.46 \%\end{aligned}$$

3. Figures

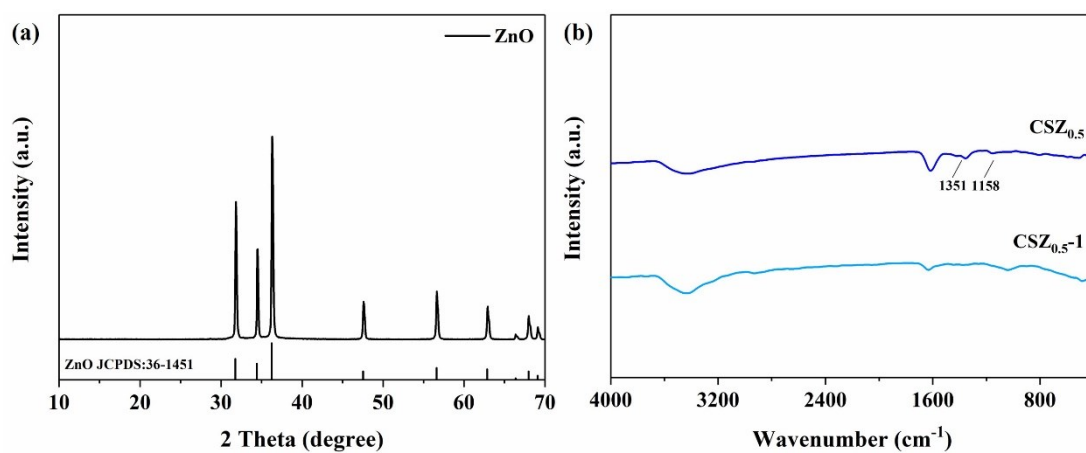


Fig. S1. The XRD pattern of ZnO (a), FT-IR spectra of CSZ_{0.5} and CSZ_{0.5-1} (b).

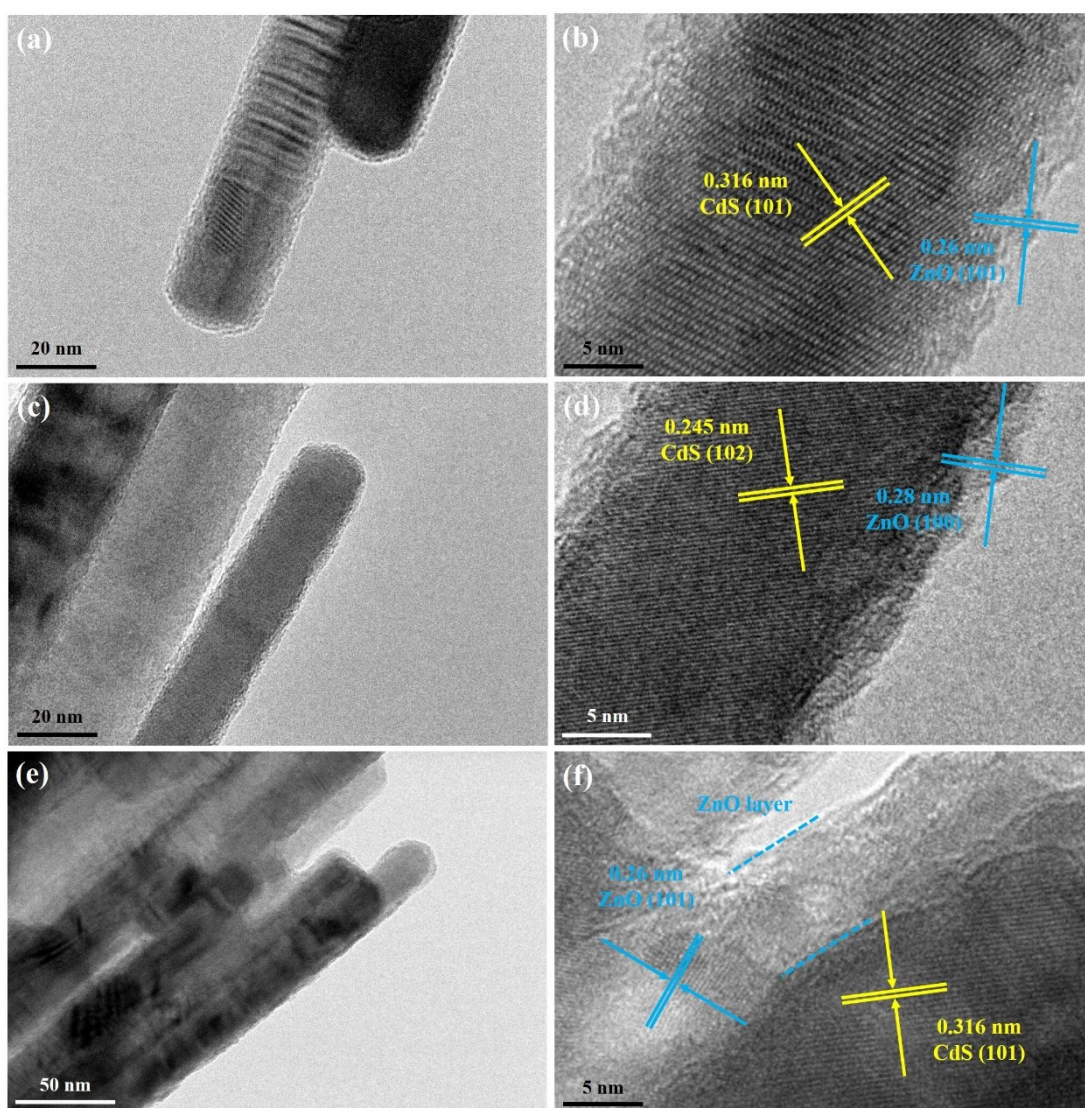


Fig. S2. TEM images of CSZ_{0.3} (a, b), CSZ₁ (c, d) and CSZ₂ (e, f).

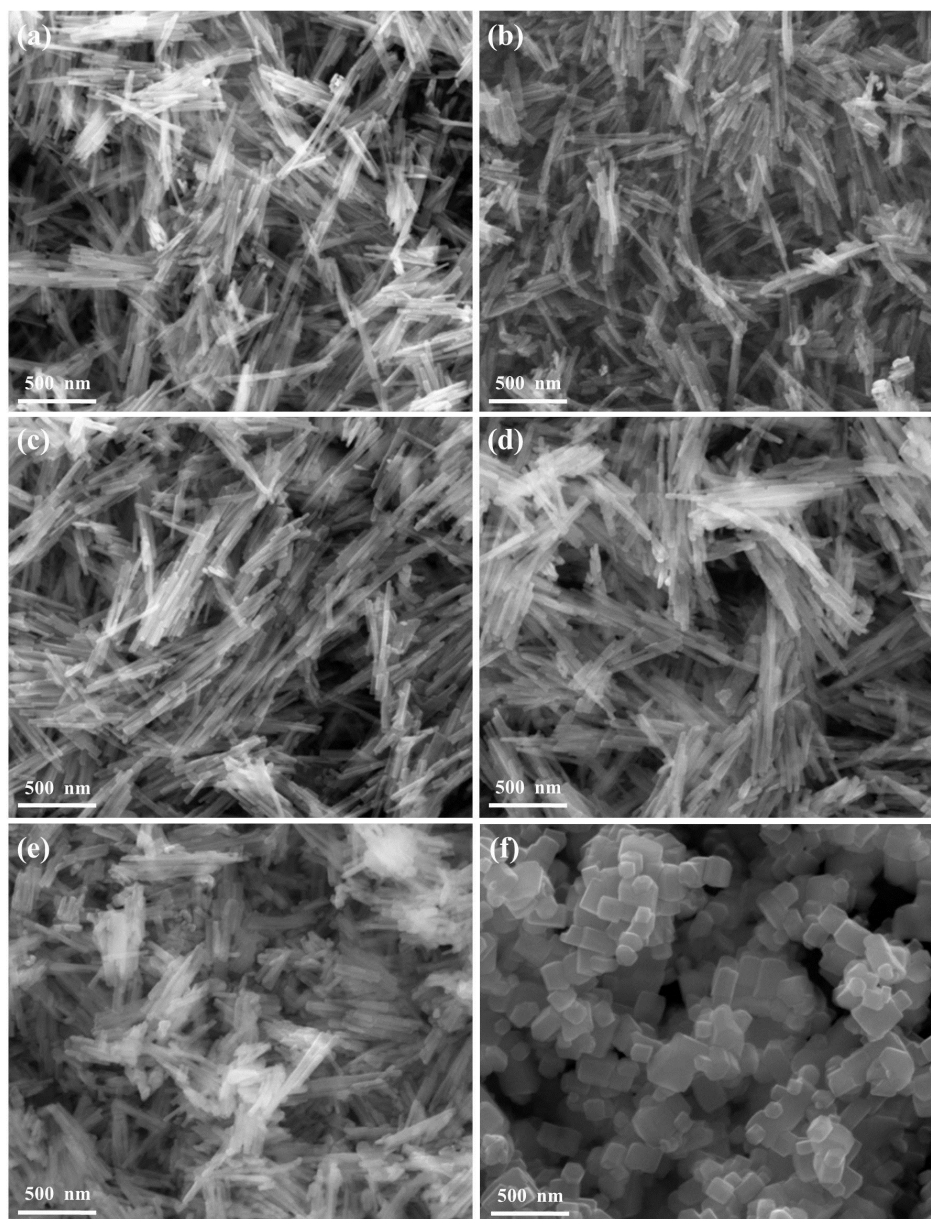


Fig. S3. SEM images of CdS (a), CSZ_{0.3} (b), CSZ_{0.5} (c), CSZ₁ (d), CSZ₂ (e) and ZnO (f).

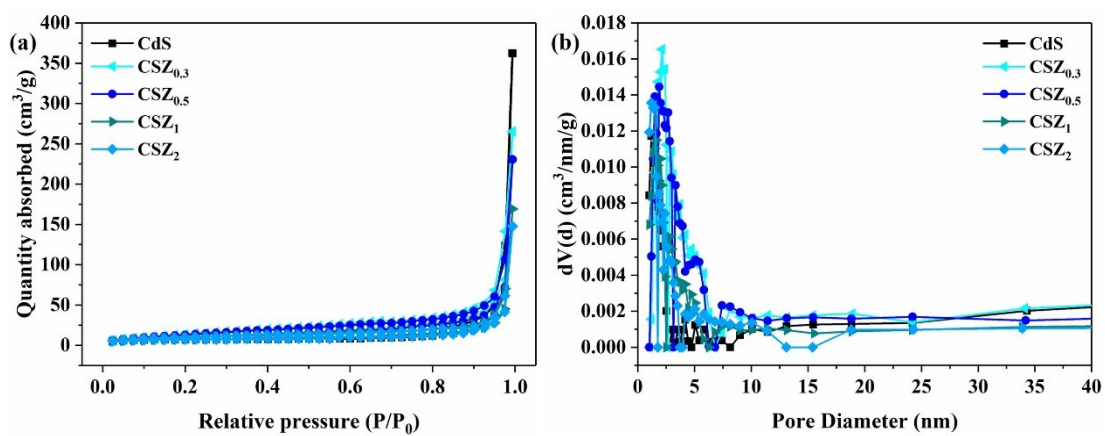


Fig. S4. N₂ adsorption-desorption isotherms (a) and pore size distribution curves (b) of the samples.

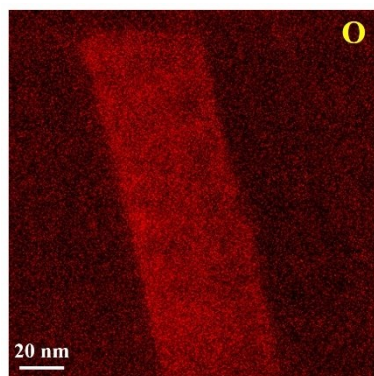


Fig. S5. The O elemental mapping of the CSZ_{0.5} sample.

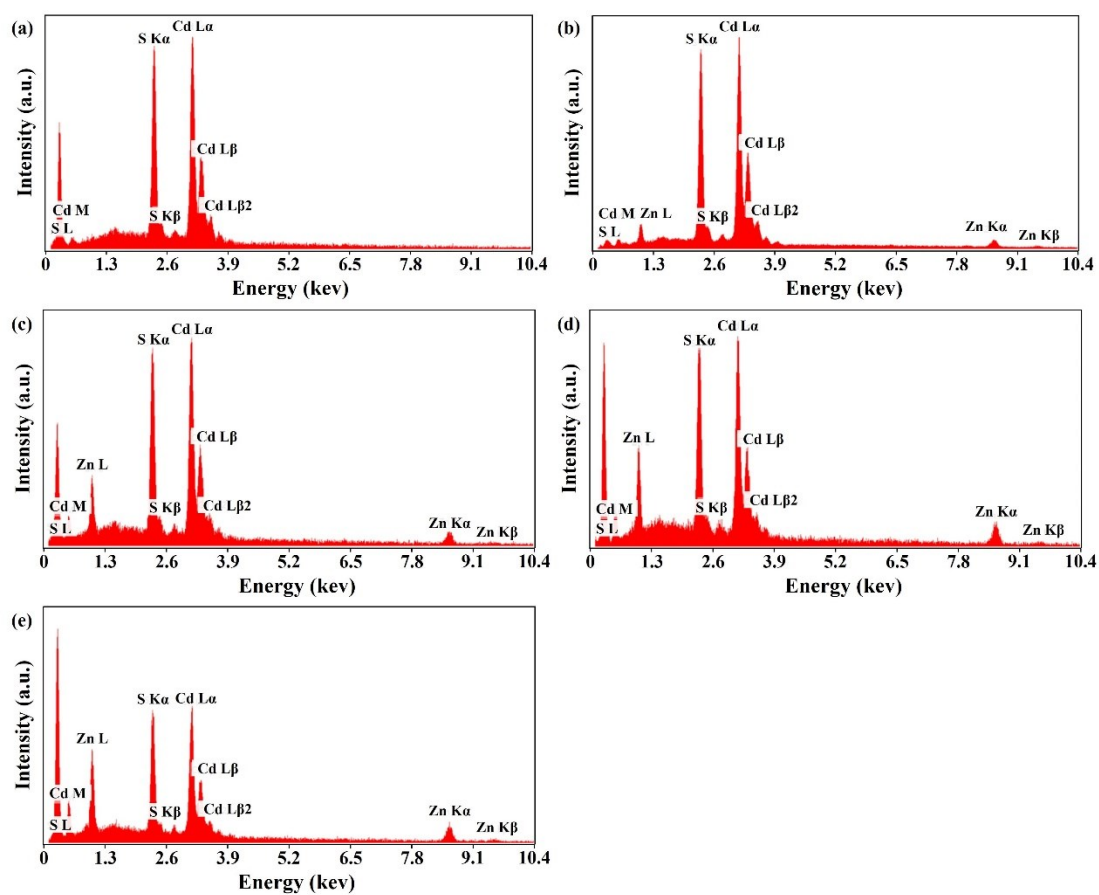


Fig. S6. EDX spectra of CdS (a), CSZ_{0.3} (b), CSZ_{0.5} (c), CSZ₁ (d) and CSZ₂ (e).

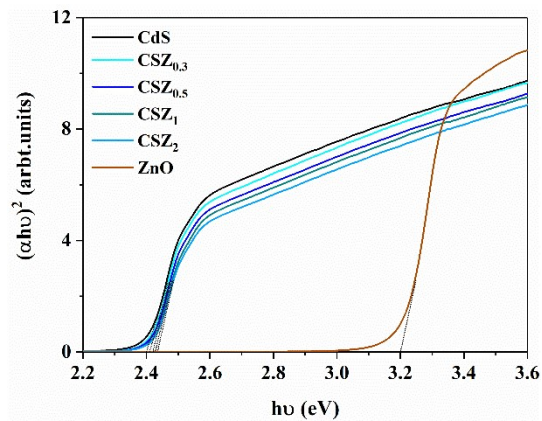


Fig. S7. Tauc plots of the as-prepared samples.

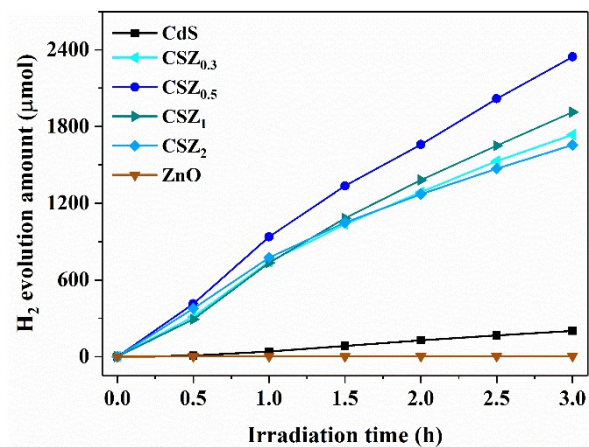


Fig. S8. Time courses of H₂ evolution over the as-synthesized samples.

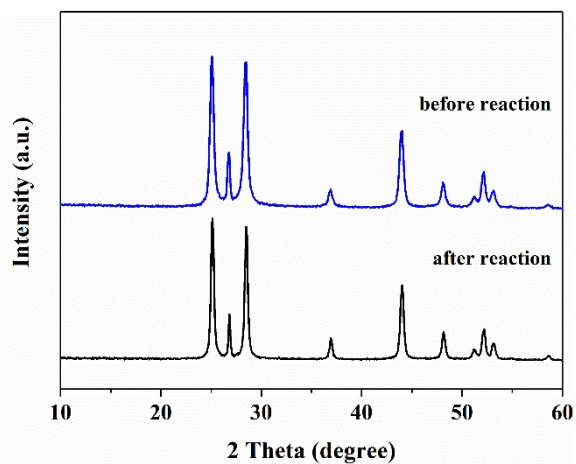


Fig. S9. XRD patterns of the CSZ_{0.5} sample before and after cycling tests.

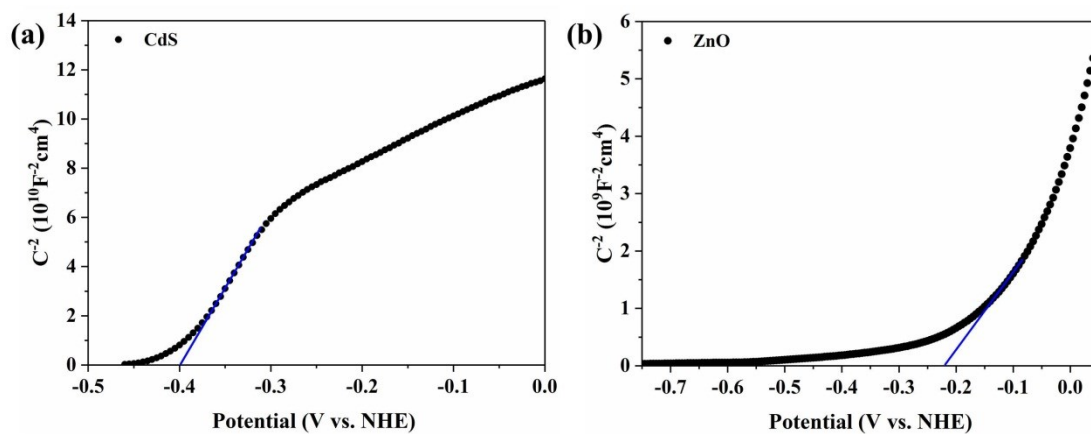


Fig. S10. Mott-Schottky plots of CdS with E_{fb} of about -0.40 eV (a), ZnO with E_{fb} of about -0.22 eV (b) versus NHE.

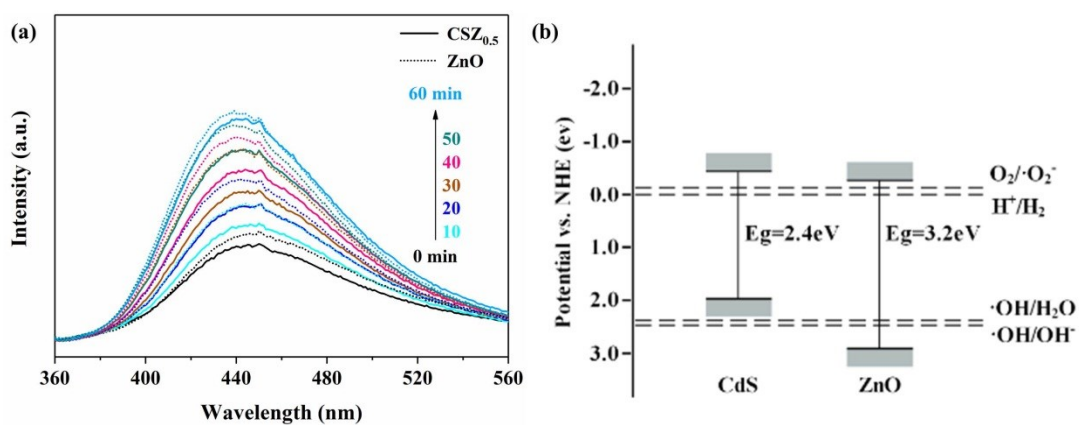


Fig. S11. PL spectra (a) of $CSZ_{0.5}$ (continuous line) and ZnO (dotted line) sample in a TA solution irradiated by simulated sunlight at different irradiation time (at the excitation wavelength of 315 nm), and the schematic diagram (b) of the band positions of CdS and ZnO.

4. Tables

Table S1 The specific surface areas (S_{BET}) of the as-synthesized samples.

Sample	CdS	CSZ _{0.3}	CSZ _{0.5}	CSZ ₁	CSZ ₂
S_{BET} (m ² /g)	24.32	39.05	36.93	25.27	23.46

Table S2 The percentages of Cd, S and Zn in the as-prepared samples measured by EDX.

Sample	CdS	CSZ _{0.3}	CSZ _{0.5}	CSZ ₁	CSZ ₂
S K (at. %)	54.54	50.18	49.13	46.41	45.15
Cd L (at. %)	45.46	41.50	39.38	35.26	34.15
Zn K (at. %)	-	8.32	11.49	18.33	20.7
Zn/Cd (%)	-	20.05	29.17	51.96	60.61

Table S3 The percentages of Cd and Zn in the as-synthesized samples measured by ICP-MS.

Sample	CSZ _{0.3}	CSZ _{0.5}	CSZ ₁	CSZ ₂
Cd (at. %)	85.57	80.65	71.68	66.26
Zn (at. %)	14.43	19.35	28.32	33.74
Zn/Cd (%)	16.86	23.99	39.51	50.92

Table S4 The band gap values of the as-prepared samples.

Sample	CdS	CSZ _{0.3}	CSZ _{0.5}	CSZ ₁	CSZ ₂	ZnO
Band gap (eV)	2.40	2.41	2.42	2.43	2.44	3.20

Table S5 Comparison of the photocatalytic H₂ evolution rates over different CdS-based

photocatalysts.

Catalyst	R(H ₂) (mmol/g/h)	Sacrificial agents	Reference
CdS NRs	22.3	0.35 M Na ₂ S and 0.25 M Na ₂ SO ₃	This work
CSZ _{0.5}	268.5	0.35 M Na ₂ S and 0.25 M Na ₂ SO ₃	This work
Pt-PdS/CdS	29.23	0.5 M Na ₂ S and 0.5 M Na ₂ SO ₃	[1]
Pd/CdS/PdS	89.2	0.1 M Na ₂ S and 0.1 M Na ₂ SO ₃	[2]
CdS/Ni ₂ P	85.0	0.25 M Na ₂ S and 0.35 M Na ₂ SO ₃	[3]
CdS/ZnO/PdS	98.82	0.35 M Na ₂ S and 0.25 M Na ₂ SO ₃	[4]
CdS/Au	2.192	0.35 M Na ₂ S and 0.25 M Na ₂ SO ₃	[5]
Au/CdS/PdS	16.35	0.35 M Na ₂ S and 0.25 M Na ₂ SO ₃	[6]
CdS/MoS ₂	9.73	0.35 M Na ₂ S and 0.25 M Na ₂ SO ₃	[7]
CdS/Co ₃ N	137.33	0.75 M Na ₂ S and 1.05 M Na ₂ SO ₃	[8]
CdS/MoS ₂	6.1	0.35 M Na ₂ S and 0.35 M Na ₂ SO ₃	[9]
CdS/ZnS/PdS	102.1	0.35 M Na ₂ S and 0.25 M Na ₂ SO ₃	[10]

Table S6 AQE over the CSZ_{0.5} sample at different wavelengths.

λ (nm)	365	380	420	500
AQE (%)	34.46	20.39	5.51	3.78

Table S7 Apparent quantum efficiency of CdS-based photocatalysts for hydrogen evolution.

Catalyst/weight	Light source	Wavelength h	Sacrificial agent	AQE	Reference
CSZ _{0.5} /20 mg	225 W lamp	365 nm	Na ₂ S and Na ₂ SO ₃	34.46 %	This work
CSZ _{0.5} /20 mg	225 W lamp	380 nm	Na ₂ S and Na ₂ SO ₃	20.39 %	This work
Pt-PdS/CdS/300 mg	300 W lamp	420 nm	Na ₂ S and Na ₂ SO ₃	93 %	[1]
CdS/ZnS/PdS/50 mg	225 W lamp	365 nm	Na ₂ S and Na ₂ SO ₃	26.1 %	[10]
CdS/Pt/20 mg	300 W lamp	435 nm	Na ₂ S and Na ₂ SO ₃	10.4 %	[11]
CdS/NiO/200 mg	500 W lamp	420 nm	Na ₂ S and Na ₂ SO ₃	6.02 %	[12]
CdS/NiS/50 mg	300 W lamp	420 nm	Na ₂ S and Na ₂ SO ₃	6.1 %	[13]
CdS/TiO ₂ /100 mg	350 W lamp	420 nm	Na ₂ S and Na ₂ SO ₃	8.9 %	[14]
Zn _{0.3} Cd _{0.7} S/ReS ₂ /20 mg	300 W lamp	400 nm	Na ₂ S and Na ₂ SO ₃	23.24 %	[15]
WO _{3-x} /Zn _{0.3} Cd _{0.7} S/100 mg	300 W lamp	420 nm	Na ₂ S and Na ₂ SO ₃	7.3 %	[16]

Table S8 The concentration of Cd²⁺ in solution measured by ICP-MS.

Sample	CdS	CSZ _{0.5}	CSZ _{0.5}
Irradiation time (h)	3	3	18
Cd ²⁺ concentration (mg/L)	1.22	0.008	0.31

Table S9 Fluorescence lifetimes of the CdS and CSZ_{0.5} sample.

Sample	τ_1 (ns)	A_1 (%)	τ_2 (ns)	A_2 (%)	τ_3 (ns)	A_3 (%)	τ_4 (ns)
CdS	0.4236	49.79	2.9282	39.72	15.7631	10.49	9.76
CSZ _{0.5}	0.4039	66.27	2.7495	28.66	13.9000	5.08	6.86

5. Density functional theory (DFT) calculations

We performed the first principles calculations based on density functional theory (DFT) for all relevant structures using the plane wave basis under the periodic boundary conditions (PBCs), as implemented in VASP software suit.¹⁷ The projector augmented wave (PAW) method was employed to describe the interactions between valence shells and the ionic core. The valence electron configurations were Zn ($3d^{10}4s^2$), Cd ($4d^{10}5s^2$), S ($3s^23p^4$), O ($2s^22p^4$), C ($2s^22p^2$) and H($1s^1$), respectively. In order to properly describe various chemical bonds in the modelling structures as well as the weak van der Waals interactions between absorbent and substrate, the SCAN-rVV10 exchange-correlation density functional was used in all calculations.¹⁸⁻²⁰ For the modelling structure involving the transition metals such as Zn and Cd, the electron-electron correlation effects may not be sufficiently captured by the semi-local density functional such as the meta-generalized gradient approximation (meta-GGA) in terms of SCAN functional. One of the most widely used remedies to the issue is the introduction of DFT+U method in the structural optimization and energy calculations. In this paper, we adopted SCAN-rVV10+U methodology, and the strong on-site Coulomb interactions among those highly localized 3d electrons were taken into account by applying an effective parameter $U = 4.7$ eV for Zn element.²¹ The effects of the likely magnetism on the thermodynamics of HER were also properly included in all spin-polarized first principles calculations. The plane wave expansion in reciprocal space was conducted by using a kinetic energy cutoff value of 400 eV. Regarding the k-mesh in Brillouin zone, we only employed the Γ -point in all calculations, because the dimensions of supercell models were all larger than 12 Å. Using the current computational parameters, the total energy was converged to 10^{-4} eV/cell or 10^{-6} eV/atom. In addition, the mean atomic force was reduced to 0.05×10^{-3} eV/Å.

Here, we are mainly interested in the adsorption free energy of a single H atom on the core-shell like hetero-structures consisting of CdS substrate and ZnO over layer with and without the adsorption of the ascorbic molecule (AA), i.e., CdS/ZnO and CdS/ZnO-AA. As indicated by the notations of the supercell models, the AA molecule was chemically absorbed on the surface of ZnO over layer. Although the experimental TEM images (**Fig. 1** and **Fig. S2**) implied that the ZnO shell may completely cover the substrate CdS core, forming the perfect core-shell like structure, the ZnO over layer only partially deposited on the substrate to investigate the influences of ZnO shell on the adsorption free energies at the available adsorption sites for both core and shell materials.

In the case of CdS/ZnO heterostructure, we first cut the 3×3 slab model for (100) surface of CdS from optimized crystal structure by DFT. The ratio of Cd/S in the slab model was 1:1, and which is exactly the same as that of CdS bulk phase. The total number of atoms in the slab was 90, i.e., $\text{Cd}_{45}\text{S}_{45}$ or $(\text{CdS})_{45}$. For the ZnO shell, the (0001) surface can be terminated by either O or Zn atom, and which represents a polar surface. The polar surface is thermodynamically unstable due to the presence of large surface dipole moments (symmetric cut) or bulk dipole moments (asymmetric cut). Therefore, we excluded the possible heterostructures involving ZnO (0001) surface, i.e., ZnO (0001) // CdS (100). Instead, we built a 4×3 slab model of the non-polar (100) surface for ZnO as the over layer deposited onto CdS surface. Therefore, orientations of the resulting CdS/ZnO interface could be denoted as CdS (100) // ZnO (100), CdS [001] // ZnO [001] and CdS [010] // ZnO [010]. We should note that (3×3) CdS (100) // (4×3) ZnO (100) supercell represents a perfect CdS/ZnO core-shell hetero-structure, i.e., no fresh CdS surface is exposed to the vacuum in the supercell. For our purpose, the (3×3) CdS (100) // (4×3) ZnO (100) modeling structure was further modified to (3×3) CdS (100) // (4×1.5) ZnO (100), referring to a heterostructure which is only

partially (50% of total surface area of CdS substrate to be precisely) covered by the ZnO over layer. Similar to the slab model of CdS substrate, the Zn/O ratio of ZnO overlayer was also fixed to that of bulk phase. The total number of atoms in the (4×1.5) ZnO (100) slab was 64 or Zn₃₂O₃₂. In **Fig. S12**, the atomic structure of (3×3) CdS (100) // (4×1.5) ZnO (100) supercell model ((CdS)₄₅(ZnO)₃₂) is illustrated.

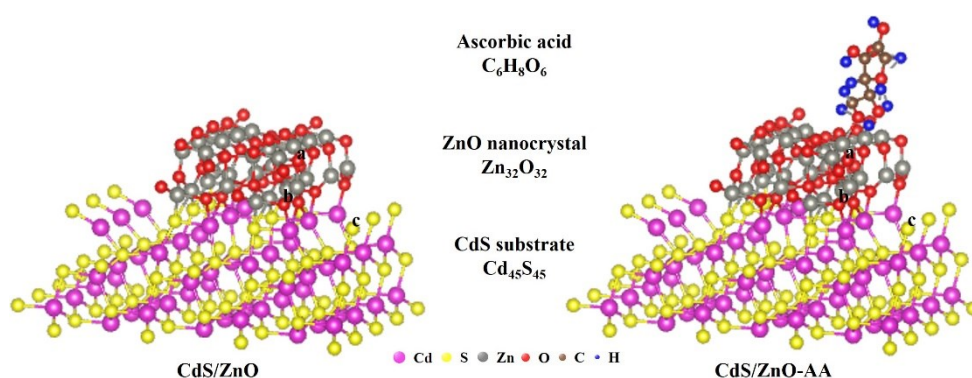


Fig. S12. The atomic structures of the supercell models of (3×3) CdS (100) // (4×1.5) ZnO (100) (left) and (3×3) CdS (100) // (4×1.5) ZnO (100)-AA (right) and different adsorption sites (a, b and c) for H* on both ZnO and CdS surfaces.

For CdS/ZnO-AA structure, a single ascorbic molecule (C₆H₉O₆) was attached to the remaining surface of ZnO overlayer in the (3×3) CdS (100) // (4×1.5) ZnO (100) supercell. Specifically, the two hydroxyl groups of ethyl motif in ascorbic molecule were docked to the two five-fold coordinated Zn atoms on ZnO (100) surface (See **Fig. S12** for the details of the atomic structure). The resulting (3×3) CdS (100) // (4×1.5) ZnO (100)-AA modelling structure, which totally has 175 atoms, was referred to (CdS)₄₅(ZnO)₃₂(C₆H₉O₆).

The adsorption energies of a single H atom at various adsorption sites on the surfaces of both CdS/ZnO and CdS/ZnO-AA were calculated from Eq. (S1) at 0 K.

$$\Delta E(*H) = E(*H) - E(*) - \frac{1}{2}E(H_2) \quad (1)$$

Where, $E(*H)$ and $E(*)$ represent the total energies of the substrate with and without H atom, respectively. The total energy of a H_2 molecule is given by $E(H_2)$. At the room temperature, the correction (entropy of H_2 molecule) to the adsorption energy results in the adsorption free energy, and which is obtained from Eq. S2.

$$\Delta G(*H) = \Delta E(*H) + 0.24 \text{ eV} \quad (2)$$

In our calculations, we have mapped the adsorption energies at various possible adsorption sites on both ZnO and CdS surfaces as well as those available sites at the ledge of ZnO overlayer.

References

- 1 H. Yan, J. Yang, G. Ma, G. Wu, X. Zong, Z. Lei, J. Shi and C. Li, *J. Catal.*, 2009, **266**, 165-168.
- 2 Q. Sun, N. Wang, J. Yu and J. C. Yu, *Adv. Mater.*, 2018, **30**, 1804368.
- 3 Z. Sun, H. Zheng, J. Li and P. Du, *Energy Environ. Sci.*, 2015, **8**, 2668-2676.
- 4 D. Ma, J.-W. Shi, Y. Zou, Z. Fan, X. Ji, C. Niu and L. Wang, *Nano Energy*, 2017, **39**, 183-191.
- 5 P. Wang, Y. Sheng, F. Wang and H. Yu, *Appl. Catal., B*, 2018, **220**, 561-569.
- 6 X.-l. Li, G.-q. Yang, S.-s. Li, N. Xiao, N. Li, Y.-q. Gao, D. Lv and L. Ge, *Chem. Eng. J.*, 2020, **379**, 122350.
- 7 Y. Li, L. Wang, T. Cai, S. Zhang, Y. Liu, Y. Song, X. Dong and L. Hu, *Chem. Eng. J.*, 2017, **321**, 366-374.
- 8 H. Chen, D. Jiang, Z. Sun, R. M. Irfan, L. Zhang and P. Du, *Catal. Sci. Technol.*, 2017, **7**, 1515-1522.

- 9 K. Chang, Z. Mei, T. Wang, Q. Kang, S. Ouyang and J. Ye, *ACS Nano*, 2014, **8**, 7078-7087.
- 10 G. Sun, S. Mao, D. Ma, Y. Zou, Y. Lv, Z. Li, C. He, Y. Cheng and J.-W. Shi, *J. Mater. Chem. A*, 2019, **7**, 15278-15287.
- 11 J. Feng, C. An, L. Dai, J. Liu, G. Wei, S. Bai, J. Zhang and Y. Xiong, *Chem. Eng. J.*, 2016, **283**, 351-357.
- 12 Z. Khan, M. Khannam, N. Vinothkumar, M. De and M. Qureshi, *J. Mater. Chem.*, 2012, **22**, 12090-12095.
- 13 J. Zhang, S. Z. Qiao, L. Qi and J. Yu, *Phys. Chem. Chem. Phys.*, 2013, **15**, 12088-12094.
- 14 D. He, M. Chen, F. Teng, G. Li, H. Shi, J. Wang, M. Xu, T. Lu, X. Ji, Y. Lv and Y. Zhu, *Superlattice. Microst.*, 2012, **51**, 799-808.
- 15 J. Huang, X. Li, X. Jin, L. Wang, Y. Deng, F. Su, P. K. Wong and L. Ye, *Mater. Adv.*, 2020, **1**, 363-370.
- 16 A. B. Yousaf, M. Imran, S. J. Zaidi and P. Kasak, *Sci. Rep.*, 2017, **7**, 6574.
- 17 G. Kresse and J. Furthmüller, *Phys. Rev. B*, 1996, **54**, 11169-11186.
- 18 J. Sun, A. Ruzsinszky and J. P. Perdew, *Phys. Rev. Lett.*, 2015, **115**, 036402.
- 19 A. Patra, J. E. Bates, J. Sun and J. P. Perdew, *P. Natl. Acad. Sci.*, 2017, **114**, E9188.
- 20 O. A. Vydrov and T. Van Voorhis, *The Journal of Chemical Physics*, 2010, **133**, 244103.
- 21 H. Peng and J. P. Perdew, *Phys. Rev. B*, 2017, **96**, 100101.